Spectrum of Light Scattering from Thermal Shear Waves in Liquids*

G. I. A. Stegeman and B. P. Stoicheff
Department of Physics, University of Toronto, Toronto, Canada
(Received 2 October 1972)

High-resolution studies of the depolarized Brillouin spectra of many molecular liquids have revealed a prominent doublet centered at the exciting frequency. The observed line shapes and intensities of the I_H^V and I_H^H polarized spectra, as well as the $\vec{k}$-vector dependence of the doublet splitting on scattering angle, are all in quantitative agreement with the theories of Leontovich, Rytov, and Volterra on light scattering from orientational motions caused by heavily damped shear waves. Analyses of the spectra on the basis of these theories have given values of the shear-wave frequencies ν_T and relaxation times τ. Values of τ in the range 3×10^{-10}–1×10^{-11} sec were obtained and τ was found to decrease with increasing temperature. Values of the shear modulus determined from ν_T and its dependence on θ were found to range from 0.6×10^8 to 9×10^8 dyn/cm^2, and to be essentially independent of temperature. Of the 27 liquids investigated, only those composed of geometrically and electrically anisotropic molecules exhibited depolarized-doublet spectra, and the resolution of the intensity minima was limited by the magnitude of the relaxation time and by the instrumental linewidth.

I. INTRODUCTION

Recent investigations of the depolarized spectra of certain liquids by Starunov, Tiganov, and Fabelinskii[1] and by Stegeman and Stoicheff[2] have led to the identification of a new propagating mode in liquids, namely, thermally excited shear waves. High-resolution Brillouin spectra revealed broad depolarized doublets with intensity minima at the exciting frequency and with peak separations of a few GHz. In the present paper we report on the results of detailed studies of the depolarized spectra of 27 liquids having different physical properties. Our observations of the angular dependence of the doublet separation, the polarization characteristics, line shapes, and intensities of the spectra confirm the initial interpretation[1] that such spectra originate from nonoscillatory thermal shear waves.

The reaction of a material to a shearing stress is one of the characteristics which distinguishes a liquid from a solid. An elastic deformation is induced when a shearing stress is applied to a solid. However, the response of a liquid to a shear stress is time dependent: Viscous flow occurs if the stress is applied slowly, but an elastic deformation can be induced by applying a stress in a sufficiently short time. It is therefore assumed that a characteristic relaxation time τ delineates the region of viscous flow from that of elastic response. For times shorter than τ a fluid may possess viscoelastic properties similar to those of an isotropic solid. Just such a property, the shear rigidity, has been measured previously for highly viscous[3] ($\eta\sim10^7$ poise) and supercooled[4] liquids using ultrasonic techniques in which a transverse wave is generated by appropriate transducers. For these liquids the relaxation times are of the order of milliseconds. For less viscous and nonassociated liquids, the characteristic relaxation times are expected to be many orders of magnitude shorter. In simple liquids, the existence of high-frequency phonons which correspond to a real value of the shear modulus had been suggested by Brillouin.[5] He noted that the small difference between the specific heat of a solid and the corresponding liquid could be understood only if transverse excitations known to exist in solids persisted in the liquid state.

A theory of light scattering by transverse fluctuations or shear waves in liquids was given by Leontovich.[6] He assumed that local strains in a fluid are relieved by the collective reorientation of individual molecules (assumed to be geometrically and electrically anisotropic). Rytov[7] examined the problem within the framework of the general viscoelastic theory of isotropic media and introduced frequency-dependent shear moduli and photoelastic constants. The recent observation of light scattering by thermal shear waves has led to a reformulation of the theory by Volterra[8] in which both molecular reorientation and diffusion are effective in relieving local strains. However, both the Leontovich and Volterra theories can be shown to be special cases of the more general Rytov theory.

According to the Rytov theory, light scattering from thermal shear waves gives rise to a doublet in the depolarized spectrum when the electric vectors of the incident and scattered fields are orthogonal to each other and one of the vectors is in the plane of scattering. The doublet is centered at the exciting frequency and the peaks occur at shifts of approximately $\pm\nu_T$, where ν_T is the shear-wave frequency and is related to the scattering angle by the well-known Brillouin equation. An additional contribution arising from random molecular fluctuations and having a Lorentzian profile is also predicted for the same depolarized spectrum. A

different doublet which is of very low intensity may appear in the depolarized spectrum when the planes of polarization of the incident and scattered fields are in the plane of scattering. In this case the peaks occur at shifts near those of the longitudinal Brillouin components. A brief review of Rytov's theory with the derivation of the pertinent equations describing the spectrum of scattered light will be given in Sec. II.

The apparatus which has made possible the observation of the shear-wave doublets will be described in Sec. III. The depolarized spectra of 27 molecular liquids will be presented and discussed in Sec. IV. Of these, 22 showed evidence of depolarized doublets. The correspondence between the observed spectra and the predictions of the Rytov theory is established by detailed studies of the angular dependence of the doublet separation, by line-profile comparisons, and by the identification of the weaker doublets observed near the Brillouin frequencies for longitudinal waves. As a consequence of the good agreement between the observed and predicted spectra it has been possible to evaluate the shear-wave frequency, the shear modulus of rigidity, and the relaxation time for shear-wave propagation for 22 molecular liquids. Also, in Sec. IV the temperature dependence of the shear frequency and relaxation time is presented. A summary of the general characteristics of the shear-wave spectra and of the derived quantities is given in Sec. V. In Sec. VI is a discussion of the physical and experimental factors determining the existence and observation of shear waves. Finally, in Sec. VII is included a brief summary of relaxation times obtained from other light-scattering experiments and from related dielectric-relaxation and nuclear-magnetic-relaxation measurements, for comparison with the values obtained in the present investigations.

II. RESUME OF THEORY

The most useful theory available at the present time is that due to Rytov[7] and it will be briefly reviewed here. His theory can be adapted to any relaxation mechanism and, as already mentioned, it is a more general theory than that of Leontovich or Volterra.

Rytov assumes at the very outset a frequency-dependent shear modulus for the general stress-strain relation of a small-volume element in a fluid. He thus ensures that shear waves will be included in the high-frequency excitation modes of a liquid. He further assumes coupling of fluctuations in the dielectric constant to fluctuations in the strain by means of photoelastic constants. The frequency spectrum of depolarized scattered light is directly proportional to the anisotropic strain-strain correlation function and Rytov shows that it contains two doublets, one arising from shear waves, the other from the coupling between anisotropy fluctuations and longitudinal waves, and a Lorentzian component which is characteristic of random rotational motion (or "noise") in a liquid.

According to the theory of viscoelasticity,[9] the equation of motion

$$\rho \frac{\partial^2 s_\alpha}{\partial t^2} = \sum_{\beta=1}^{3} \frac{\partial \sigma_{\alpha\beta}}{\partial x_\beta} \tag{1}$$

describes the displacement $s_\alpha(x_1, x_2, x_3, t)$ of a small-volume element of the fluid, originally situated at (x_1, x_2, x_3). Here ρ is the density and $\sigma_{\alpha\beta}$ is the stress tensor. The strain $\hat{u}_{\alpha\beta}$ induced by the stress is defined by the equation

$$\hat{u}_{\alpha\beta} = \frac{1}{2}\left(\frac{\partial s_\alpha}{\partial x_\beta} + \frac{\partial s_\beta}{\partial x_\alpha}\right) . \tag{2}$$

For convenience, the strain tensor is divided into an isotropic scalar $u = \vec{\nabla} \cdot \vec{s}$ and an anisotropic tensor of zero trace, $u_{\alpha\beta} = \hat{u}_{\alpha\beta} - \frac{1}{3} u \delta_{\alpha\beta}$. The relation between the stress and the strain is given by

$$\sigma_{\alpha\beta} = 2\mu u_{\alpha\beta} + \kappa u \delta_{\alpha\beta} . \tag{3}$$

Here μ and κ are the frequency-dependent shear and bulk moduli, respectively. For high frequencies ($\omega\tau \gg 1$), the system of Eqs. (1)–(3) has two solutions: One corresponds to longitudinal or pressure waves of velocity $[(2\mu_\infty + \kappa)/\rho]^{1/2}$ and the other to shear or torsional waves of velocity $(\mu_\infty/\rho)^{1/2}$. As a first approximation, the simplest possible form for μ, which still retains the proper low-frequency characteristics, is assumed, namely,

$$\mu = \mu_\infty i\omega\tau/(1 + i\omega\tau) , \tag{4}$$

where μ_∞ is the high-frequency shear modulus. At low frequencies ($1 \gg \omega\tau$),

$$\mu = \omega^2\tau^2\mu_\infty + i\omega\tau\mu_\infty \tag{5}$$

and the imaginary part is identified as $\omega\eta$, where η is the shear viscosity and $\mu_\infty = \eta/\tau$. At high frequencies, $\mu = \mu_\infty$ and the liquid resembles an isotropic solid in its reaction to a shear stress.

The assumed relation for μ given in Eq. (4) finds justification in the theories of Leontovich and Volterra. Leontovich assumes that the local strain in a liquid is relieved by the reorientation of molecules. A reorientation tensor $\xi_{\alpha\beta}$ is defined with the following properties. For a completely random distribution of molecules in a small-volume element of the fluid, $\xi_{\alpha\beta} = 0$. But, if a strain is applied, the molecules (assumed to be mechanically and electrically anisotropic) align preferentially so as to relieve the stress and $\xi_{\alpha\beta} \neq 0$. This preferential alignment then randomizes in a time characteristic of the reorientation time of the molecules. For a shear stress $\sigma_{\alpha\beta}$,

$$\sigma_{\alpha\beta} = 2\mu_\infty(u_{\alpha\beta} - \xi_{\alpha\beta}) .$$

The rate at which the tensor $\xi_{\alpha\beta}$ reacts to an applied stress is directly proportional to the magnitude of the stress and varies inversely as the characteristic reorientation time τ,

$$\dot{\xi} = (1/2\mu_\infty\tau)\sigma_{\alpha\beta}.$$

This leads directly to a stress-strain relation defined by

$$\sigma_{\alpha\beta} = 2\mu_\infty [i\omega\tau/(1+i\omega\tau)]u_{\alpha\beta}.$$

The shear modulus μ is identical to that assumed by Rytov [Eq. (4)] and the time τ is identified with molecular reorientation.

The theory of Volterra assumes that the local strain can be relieved not only by reorientation, but also by molecular diffusion. Volterra defines a vector $\vec{h}(x_1, x_2, x_3, t)$ which describes the equilibrium position of a small-volume element at time t. The shear strain $u_{\alpha\beta}$ defined previously now refers only to the equilibrium position at time $t=0$. The elastic shear strain at any time t is

$$w_{\alpha\beta} = u_{\alpha\beta} - H_{\alpha\beta} = \sigma_{\alpha\beta}/2\mu_\infty.$$

$H_{\alpha\beta}$ is a tensor defined in analogy to $u_{\alpha\beta}$ as

$$H_{\alpha\beta} = \frac{1}{2}\left(\frac{\partial h_\alpha}{\partial x_\beta} + \frac{\partial h_\beta}{\partial x_\alpha}\right).$$

The rate of molecular rearrangement depends on the magnitude of the stress and is given by

$$\dot{H}_{\alpha\beta} = (1/2\mu_\infty\tau)\sigma_{\alpha\beta}.$$

These relations again give exactly the same form for μ as assumed by Rytov, but τ in this case is determined by the rate of molecular diffusion.

The theories of Leontovich and Volterra, when extrapolated to the limit of constant viscous flow, predict

$$\sigma_{\alpha\beta} = -\mu_\infty\tau\frac{\partial v_\alpha}{\partial x_\beta},$$

where $\vec{v}$ is the velocity of a volume element. Since this relation defines the macroscopic viscosity η, then for all temperatures, $\eta = \mu_\infty\tau$.

Any process which induces changes in the local molecular polarizability or in the dielectric constant of the bulk medium gives rise to light scattering. Rytov assumes that fluctuations in the dielectric tensor $\epsilon_{\alpha\beta}$ are coupled to fluctuations in the isotropic strain u and the anisotropic strain $u_{\alpha\beta}$ as follows:

$$\epsilon_{\alpha\beta} = Yu\delta_{\alpha\beta} + Xu_{\alpha\beta}. \tag{6}$$

(Note that changes in $\epsilon_{\alpha\beta}$ owing to fluctuations in the temperature are ignored as they give rise to negligible scattering.) Here X and Y are photoelastic constants (and in an isotropic solid correspond to the P_{44} and P_{11} Pockel coefficients, respectively). The constant Y relates fluctuations in the density to changes in the refractive index and is usually only weakly dependent on frequency. The polarized Brillouin triplet originates from this first term in Eq. (6) and reflects the frequency spectrum of fluctuations in the local density. The second term $Xu_{\alpha\beta}$ leads to depolarized scattering. The photoelastic constant X defines the change in the dielectric constant of a liquid when a shearing force is applied. Since the reaction of a liquid to a transverse stress is frequency dependent, then so also is X. As a result, the depolarized frequency spectrum depends on the fluctuation spectrum of both shear strain and anisotropy. Rytov assumes that $X \propto \mu$ since both X and μ are related to the relaxation of a shear stress in a liquid and thus the shear and anisotropy relaxation times, τ_μ and τ_X, respectively, are assumed to be equal.

Consider now a radiation field of frequency ω_0 and electric vector E_β polarized in the β direction, incident on the scattering volume. It induces a dipole moment P_α given by

$$P_\alpha = \epsilon_{\alpha\beta}E_\beta/4\pi, \tag{7}$$

where $\epsilon_{\alpha\beta}$ is the fluctuation in the dielectric constant of the medium about the average value ϵ_0. The frequency spectrum of light radiated by the dipole P_α, observed normal to P_α, is

$$I(\omega) = \text{const} \times |P_\alpha(\omega, q)|^2. \tag{8}$$

The constant contains the usual ω_0^4 dependence on frequency and $1/R^2$ dependence on the distance between the scattering volume and the detector. Here, ω is the frequency of the fluctuations in $P_\alpha(\omega, q)$, as well as the frequency shift of the scattered radiation from the incident frequency. The wave vector $\vec{q}$ of the fluctuations is related by $\vec{q} = \vec{k}_0 - \vec{k}_s$ to the wave vectors $\vec{k}_0$ and $\vec{k}_s$ of the incident- and scattered-light fields, respectively. For frequencies such that $\omega_0 \gg \omega$, the Brillouin equation

$$q = 2k_0 \sin\tfrac{1}{2}\theta \tag{9}$$

relates q to the scattering angle θ (measured relative to the direction of the incident beam). By substituting Eqs. (6) and (7) into (8), the following expression for the depolarized spectrum is derived:

$$I(\omega) \propto |\bar{X}|^2 \times u_{\alpha\beta}(\omega, q)u^*_{\alpha\beta}(\omega, q).$$

In order to compute the depolarized spectrum of scattered light it is necessary to evaluate the anisotropic strain autocorrelation function. Rytov has done this for $u_{\alpha\beta}$ and u using standard "fluctuation theory."[10] It is meaningful to separate the $u_{\alpha\beta}u^*_{\alpha\beta}$ correlation function into two parts: one which satisfies Eqs. (1)–(3) and describes the decay of the strain fluctuations into the two normal phonon modes; the second which originates from the "external forces" applied in the derivation and describes the random "noise" in the system.

The standard notation will be used to designate the intensity of scattered light, e.g., I_H^V, I_V^H, I_H^H. The letters V and H are used to denote radiation with the electric vector polarized normal to, and parallel to, the scattering plane, respectively. When used as subscripts these letters refer to the incident radiation and, as superscripts, the scattered radiation. The equations derived by Rytov for the depolarized spectra are

$$I_H^V = I_V^H = C\left(\frac{1}{\omega^2\tau^2+1}\sin^2\tfrac{1}{2}\theta + \frac{\omega^2}{\omega^2+\tau^2(\omega^2-\omega_T^2)^2}\cos^2\tfrac{1}{2}\theta\right) \tag{10}$$

and

$$I_H^H(\theta=90^\circ) = \frac{C}{4}\left(\frac{1}{\omega^2\tau^2+1} + \frac{3(\omega^2-\omega_L^2)}{(\omega^2-\omega_L^2)^2+\omega^2\tau^2(\omega^2-\omega_L^2-\frac{4}{3}\omega_T^2)^2}\right), \tag{11}$$

where $\omega_L = 2\pi\nu_L = (\kappa/\rho)^{1/2}q$ and $\omega_T = 2\pi\nu_T = (\mu_\infty/\rho)^{1/2}q$. Here C is a constant and ω_L (or ν_L) is the longitudinal-phonon frequency. By analogy, ω_T (or ν_T) is the shear-wave frequency and is related to the scattering angle θ by the well-known Brillouin equation $\omega_T = 2nk_0V_T\sin\frac{1}{2}\theta$, where V_T is the transverse sound velocity.

The more familiar equation derived by Rytov for the isotropic spectrum is

$$I_V^V = \frac{4}{3}C\frac{1}{\omega^2+1/\tau^2} + |Y|^2\left(\frac{1-1/\gamma}{\omega^2+1/\tau_A^2} + \frac{1/2\gamma}{(\omega-\omega_L)^2+1/\tau_L^2} + \frac{1/2\gamma}{(\omega+\omega_L)^2+1/\tau_L^2}\right). \tag{12}$$

Here γ is the ratio of the specific heats and τ_A and τ_L are the decay times for entropy and pressure fluctuations, respectively.

The I_V^H and I_H^V spectra consist of two components each centered at the exciting frequency. One is a Lorentzian line originating from scattering by random "noise" fluctuations which decay in time τ; this component vanishes in the forward direction as shown by the term $\sin^2\frac{1}{2}\theta$. The second component is a doublet originating from scattering by shear waves, and disappears in the backward direction because of the term $\cos^2\frac{1}{2}\theta$. This doublet has peaks at $\pm\omega_T$ and its width is inversely proportional to τ, which is identified as the half-life of the transverse phonons. It may be noted here that the peaks at $\pm\omega_T$ correspond to an infinite-frequency shear modulus and not to the value of the real part of the modulus at the frequency ω_T. The relative intensities of the two terms in Eq. (10) depend only on the scattering geometry: For low scattering angles $\theta<90^\circ$, the I_H^V spectrum is dominated by the doublet term, but for $\theta>90^\circ$, the Lorentzian term has the greater intensity and may shift the peak of the spectrum away from ω_T.

The I_H^H component is unique, as it represents a depolarized spectrum only at a scattering angle of 90°. At other angles, a contribution due to the polarized Brillouin triplet appears. The normal-mode term is Lorentzian, except in the limited frequency interval defined by $\omega_L^2-\omega_T^2>\omega^2>\omega_L^2+2\omega_T^2$. In this region, a doublet with peaks at $\omega=\pm(\omega_L+\frac{2}{3}\omega_T^2/\omega_L)$ occurs due to coupling between the anisotropic fluctuations and the longitudinal waves.

III. EXPERIMENTAL APPARATUS

A schematic diagram of the apparatus used in this experiment is shown in Fig. 1. In principle the apparatus is similar to that used in previous experiments performed in this laboratory and is described in detail in Ref. 11. Special attention was paid to the requirements for the present experiment as dictated by the shear-wave parameters ν_T and τ. The spectral breadth, $(2\pi\tau)^{-1}$ for depolarized scattering, is large (~5 GHz) compared to the linewidths of longitudinal Brillouin spectra. Therefore, in order to achieve reasonable signal-to-noise levels (say, 50 : 1) rather high incident-laser power is necessary (~100 mW). At the same time a narrow instrumental line must be used since the shear-wave frequency ν_T is typically ~1 GHz. A specially designed laser was used in conjunction with a high-quality Fabry–Perot interferometer to satisfy these requirements.

The He-Ne laser was 4 m long, 15 mm in diameter, and used Brewster windows to produce plane polarized light. Spherical mirrors of 10-m radii of curvature formed the cavity, with the output mirror having a transmission of ~2.5%. High output power of 50–400 mW was obtained at $\lambda=6328$ Å in a relatively narrow line: For the typical power used in the present experiments, ~100 mW, the full width at half-intensity maximum was measured to be 0.65 GHz. A dc discharge was used and the

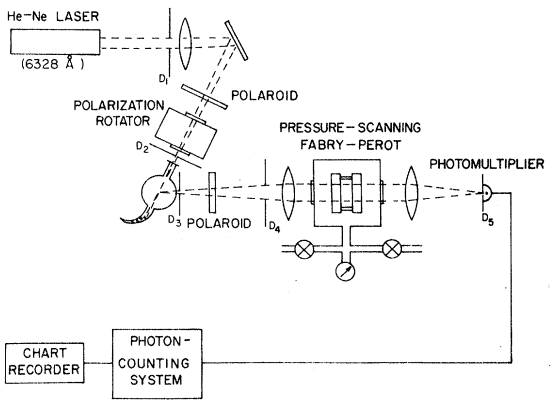

FIG. 1. Schematic diagram of the experimental apparatus.

laser power was maintained constant to ± 1% with a current- and voltage-stabilized supply.

The sample cells were of the design described in Ref. 11: They were cylindrical in shape, with a flat entrance window and with a Wood's horn to trap the transmitted laser light. The entrance tube, horn, and cylinder wall opposite the viewing area were painted with flat black paint. Stray light scattered from an empty cell was found to be highly polarized (>90%) and to contribute only 3% to the peak signal at the laser frequency for the weakest scattering liquid investigated. During an experiment the sample cell was set in a temperature-controlled copper block. For the temperature range 3–95 °C, water from a regulated bath was circulated through the block. The range down to about – 30 °C was attained by forcing evaporated nitrogen gas through the block. The entrance and viewing areas were kept free of frost by blowing dry air on the surfaces. The temperature was measured to ± 1 °C with a thermocouple immersed in the sample liquid just a few mm above the laser beam.

The liquids used were of the highest purity available and were used without further purification. To reduce sample deterioration due to ultraviolet radiation all of the liquids were stored in the dark. During experiments, especially at higher temperatures, some of the liquids changed color because of oxidation: For example, aniline changed from a pale yellow to red in a week, but the samples yielded identical doublet spectra. The liquids were rendered dust free by forcing them through 0.22-μm solvinert Millipore filters. This procedure was especially critical since the slightest amount of dust present in some samples was sufficient to completely obliterate the doublet minima.

The cylindrical cells were used for experiments with scattering angles of 45°–140°. For scattering experiments at angles near 180° a cell was constructed from Pyrex tubing 2 cm in diameter and 10 cm in length. A high-quality window was cemented at one end and a Wood's horn fused at the other. Spurious scattering at the laser frequency was eliminated by ensuring that the incident laser beam hit the horn as far off the interferometer axis as possible, and by positioning carefully a blackened screen at the front window to separate the incident and scattered beams.

In order to make true measurements of I_H^H, I_H^V, and I_V^H, the establishment of the scattering plane and the proper setting of the polaroid sheets relative to it are critical. Error in this alignment will tend to fill in the intensity minimum of the doublet expected from Eq. (10). A method based on a knowledge of the expected polarization characteristics of the scattered light was used: At exactly 90° scattering, the I_H^H spectrum does not contain the Brillouin triplet arising from isotropic scattering. A cell of carbon tetrachloride, which has a very weak depolarized spectrum relative to the Brillouin triplet intensity, was used for this alignment procedure. The interferometer was set at the laser frequency and a polarization rotator (99.995% efficient) was placed before the scattering cell. The rotator was adjusted until the scattered intensity from the sample was a minimum. This ensured an incident beam polarized in the scattering plane. Next, the light transmitted through a polaroid placed after the rotator was minimized by rotation of the polaroid. This polaroid then passed only light polarized perpendicular to the scattering plane. A second analyzing polaroid, with axis in the scattering plane, was aligned by crossing it with the first polaroid until again a minimum in the scattering intensity was obtained. (A pair of selected polaroids, each with a transmission of 70%, had an extinction ratio when crossed of 5×10^{-4}.) In this manner, the scattering plane was established and the axes of the polaroids were calibrated very accurately as each of the operations involved a sharp intensity minimum.

Precautions were taken to reduce stray laser-light scattering. A diaphragm D_1 was placed after the laser in order to reduce the spontaneous emission from the laser in the forward direction. The diaphragm D_2 reduced stray scattering off the mirror, rotator, and polaroid. Finally, only light from the center of the scattering cell was passed by the two diaphragms D_3 and D_4 between the cell and the interferometer.

The pressure-scanned Fabry–Perot interferometer has also been described previously.[11] For this experiment, the 1.5-in.-diam plates were flat to $\frac{1}{200}\lambda$ and had a reflectivity of 98.3% at the operating wavelength $\lambda = 6328$ Å. Two Invar spacers were used, of length 3.984 ± 0.002 and 9.993 ± 0.002 mm, giving spectral free ranges of 1.255 and 0.5004 cm^{-1}, or 37.65 and 15.01 GHz, respectively. Light scattered from the center of the sample cell was collected by a lens of 30-cm focal length through aperture D_4 of 1.4 cm; the latter defines the solid angle subtended at the cell center as ~0.05 sr, and limits the aperture of the interferometer plates to the central 1.4-cm diameter. The interference pattern was then focused by a high-quality lens of 50-cm focal length onto a metal screen and centered on the 1-mm circular aperture D_5, which is concentric with the interferometer axis. With this aperture, with a spacer of 4 mm, and with a laser power of ~100 mW, the total instrumental width was measured to be 0.8 GHz, resulting in a finesse of ~50.

A cooled photomultiplier (ITT FW-130) with a dark count of $\frac{1}{2}$/sec was used. Its output was analyzed by a standard photoelectron counting sys-

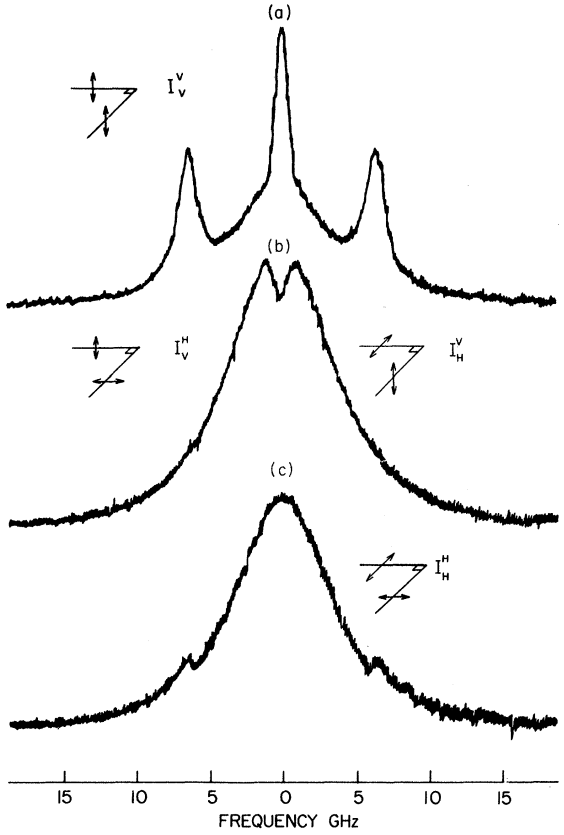

FIG. 2. Spectra of liquid quinoline (at 22 °C and for $\theta = 90°$) obtained with various polarizations of the incident and scattered radiation. Spectrum (a) is shown at half the magnification of (b) and (c).

tem consisting of preamplifier, amplifier, pulse-height analyzer, and ratemeter. The resulting spectra were displayed by a chart recorder with normally about six orders being scanned for each experiment. Also, before and after each experiment several scans of the instrumental line were recorded for use in the deconvolution of the observed spectra.

IV. OBSERVED SPECTRA AND ANALYSIS

In the course of this investigation, the depolarized spectra of 27 molecular liquids having various structures, viscosities, and dipole moments were studied. Five of these liquids exhibited only very broad spectra (or "Rayleigh wings") without any evidence of structure. All of the remaining 22 liquids displayed evidence of the shear-wave doublets discussed in Sec. II and predicted by Eqs. (10) and (11). The best-resolved doublets were observed in the spectra of quinoline, aniline, and nitrobenzene, and these will be used to illustrate the characteristic features of the depolarized spectra.

Typical spectra are reproduced in Fig. 2. These show the spectra of quinoline at 90° scattering for all possible states of linear polarization of the incident and scattered light. Figure 2(a) shows the I_V^V or total spectrum of scattered light. It consists of a central Rayleigh line and two Brillouin components (arising from thermally excited longitudinal waves) superimposed on an intense broad background. This polarized triplet accounts for only ~10% of the total integrated intensity of the I_V^V spectrum, the major contribution being due to depolarized scattering. Figures 2(b) and 2(c) demonstrate that the depolarized scattering consists of prominent and relatively narrow frequency components, in addition to the very broad "Rayleigh wing." The I_H^V (or I_V^H) spectrum consists of a pronounced doublet, symmetrically displaced about the incident frequency, with a peak separation which is substantially smaller than the breadth of the doublet. For example, for quinoline the doublet splitting is 1.90 GHz, which is smaller than the 8.4-GHz breadth (full width at half-intensity maximum) and much smaller than the 12.4-GHz separation between the longitudinal Brillouin peaks of the I_V^V spectrum. The I_H^H spectrum [Fig. 2(c)] consists of an intense single component at the incident frequency with a much less intense doublet in the wings. The breadth of the central component appears to be similar to that of the doublet in the I_H^V spectrum, and the integrated intensities of the I_H^H and I_H^V spectra are equal. All of the above observations of polarization characteristics, intensities, and line breadths are in agreement with the general predictions of Rytov's theory.

Each of the depolarized spectra is described more fully below, and detailed analyses of the observations based on Rytov's theory are given.

A. Doublet Spectrum I_H^V (and I_H^H)

The I_H^V spectrum was studied at various scattering angles from 45° to 176°. As examples, the spectra of quinoline at 45°, 90°, and 176° are shown in Fig. 3 and they are seen to be in qualitative agreement with theory. That is, the doublet structure is not evident in backward scattering, in agreement with the $\cos^2 \frac{1}{2}\theta$ intensity dependence of the doublet term in Eq. (10). Also the peak separation is observed to increase with increasing angle from 1.45 GHz at 45° to 2.03 GHz at 105°. However, in apparent disagreement with theory, the peak separation decreases to 1.87 GHz at 120°, and at 140° no doublet is observed (although the linewidth of 8.3 GHz is larger than the 7.9-GHz width measured in the backscattered spectrum). In fact, a graph of the observed peak shift ν_S plotted against $\sin\frac{1}{2}\theta$ does not yield a straight line through the origin, contrary to the prediction of Eq. (9). Such graphs for quinoline and aniline are shown in Fig. 4.

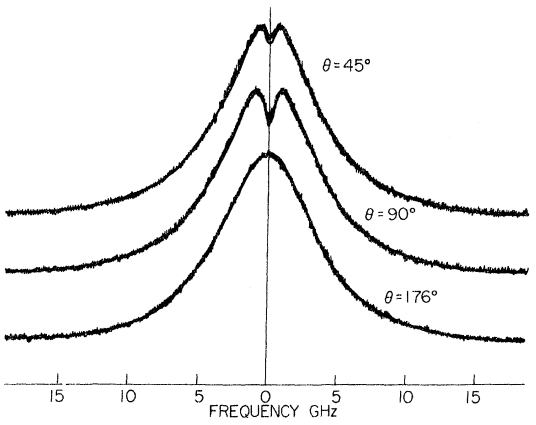

FIG. 3. I_H^V spectra of quinoline at 22 °C for the scattering angles $\theta = 45°$, 90°, 176°. The best fit to the Rytov theory is given by the solid lines.

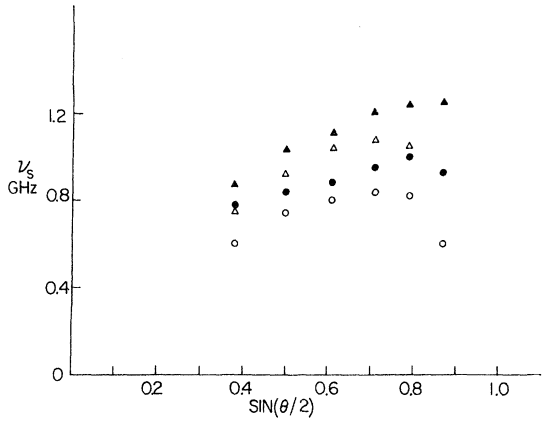

FIG. 4. Graphs of observed peak shift ν_S for quinoline (● at 22.4 °C, ○ at 4.5 °C) and aniline (▲ at 20.0 °C, △ at 3.5 °C) plotted against $\sin\frac{1}{2}\theta$.

This seeming discrepancy with theory has several causes. First, the magnitude of the instrumental width $\Delta\nu_I$ (typically ~0.8 GHz full width at half-intensity maximum) is comparable to the true shear-wave frequency ν_T. The effect on the observed spectrum is to fill in the intensity dip and to shift the peak from ν_T to higher frequencies, as shown in the computed curves of Fig. 5. Second, a closer examination of Eq. (10) shows that the Lorentzian term contributes appreciable intensity for scattering angles > 90° resulting in a shift of the peak (due to both terms) from ν_T to lower frequencies. For these reasons, it is evident that the direct measurement of the observed spectra will not yield the true shear-wave frequency ν_T nor the true line breadth Γ. Rather, it is necessary not only to use as narrow an instrumental width as possible, but also to perform extensive numerical analysis on the experimental spectra in order to determine the values ν_T and Γ.

The method of analysis is similar to that described in Ref. 11 [Sec. E(c)]. It is based on the measurement of two parameters, ν_S, the frequency shift of the peak, and $2\Gamma_S$, the full width at half-intensity maximum, directly from the observed spectra. Then the desired parameters ν_T and Γ are determined by adjusting their values in Eq. (10) until the values of ν_S and $2\Gamma_S$ from the computed spectrum agree to within ±1 MHz with the measured values. Calculations were carried out on an IBM 7094 computer. Overlap of successive interferometer orders was evaluated to frequencies at which the intensity is 0.1% of the peak intensity. For the width measurements $2\Gamma_S$, the zero of intensity was taken as the intensity minimum between adjacent orders of the interferometer. Values of ν_T and Γ obtained in this manner are listed in Tables I, II, and IV.[12]

As already mentioned, for $\theta > 90°$, the Lorentzian term in Eq. (10) dominates the I_H^V spectrum and the doublet peaks are not well defined. For these spectra, an artificial decomposition of the observed spectrum into its two components was performed. A Lorentzian line of width Γ (assumed from the I_H^H spectrum), corrected for the instrumental width, was generated and normalized to an integrated intensity of $\sin^2\frac{1}{2}\theta$ times the total intensity assigned to the doublet. This Lorentzian line was then subtracted from the observed spectrum and, for the resulting doublet, ν_S was measured and ν_T determined by fitting the new spectral profile to the doublet term in Eq. (10). Values of ν_T obtained in this way are identified by an asterisk in the tables.

A comparison of the computed spectra, for values of ν_T and Γ determined by the above analysis, with the observed spectra of Fig. 3 shows good agreement. Also, graphs of ν_T vs $\sin\frac{1}{2}\theta$ for quinoline and aniline, Fig. 6, lie on straight lines pass-

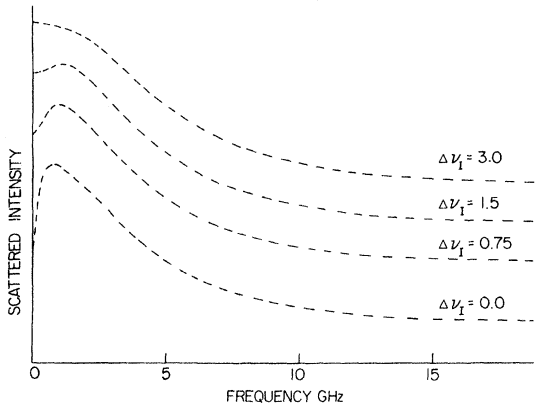

FIG. 5. Calculated I_H^V spectra of quinoline (at $\theta = 90°$) for various instrumental linewidths $\Delta\nu_I$. (Values of 0.90 and 4.14 GHz were assumed for ν_T and Γ, respectively.)

ing through the origin, in striking confirmation of the well-known Brillouin equation (9). Thus, we may conclude that the doublet spectrum has its origin in a propagating mode. However, according to the values of Γ (at $\theta = 90°$), 4.14 GHz for quinoline and 6.67 GHz for aniline, the mode is nonoscillatory and is damped out in approximately 100th of its wavelength.

B. Lorentzian Line Spectrum I_H^H

The I_H^H spectrum [Fig. 2(c)] is unique as it occurs for only one scattering angle, $\theta = 90°$. For the most part, it resembles the I_H^V backscattered spectrum with which it is compared in Fig. 7. The difference is the occurrence of a weak depolarized Brillouin doublet in the wings of the main component. This occurrence may at first sight be puzzling. However, it will be remembered that for an isotropic solid a depolarized Brillouin doublet appears in the I_H^H spectrum because of Pockel's coefficient P_{44}, which also gives rise to a shear- or transverse-wave doublet in the I_H^V spectrum of the solid. By analogy in a liquid, X replaces the coefficient P_{44}, and thus if a shear-wave doublet

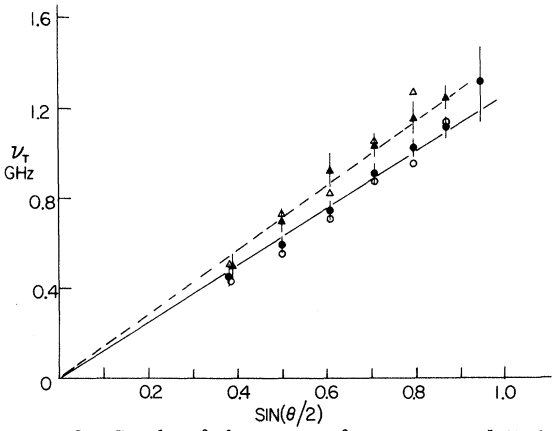

FIG. 6. Graphs of shear-wave frequency ν_T plotted against $\sin\frac{1}{2}\theta$, for quinoline (● at 22.4 °C, ○ at 4.5 °C) and for aniline (▲ at 20.0 °C, △ at 3.5 °C).

TABLE I. Shear-wave frequencies and linewidths of quinoline and aniline from I_H^V and I_H^H spectra at various scattering angles and temperatures.

Liquid and spectrum	Scattering angle θ (deg)	Instrumental linewidth $\Delta\nu_I$ (GHz)	Observed peak shift ν_S (GHz)	Observed linewidth $2\Gamma_S$ (GHz)	Shear-wave frequency ν_T (GHz)	Linewidth Γ (GHz)
Quinoline						
(T=22.4 °C) I_H^V	45	0.77 ± 0.01	0.78 ± 0.04	8.17 ± 0.13	0.46 ± 0.05	4.15 ± 0.10
	60	0.83 ± 0.02	0.84 ± 0.02	8.26 ± 0.07	0.60 ± 0.03	4.13 ± 0.05
	75	0.78 ± 0.01	0.89 ± 0.02	8.42 ± 0.05	0.75 ± 0.04	4.19 ± 0.05
	90	0.77 ± 0.02	0.95 ± 0.02	8.40 ± 0.04	0.92(0.92)*	4.13 ± 0.04
	90	0.79 ± 0.01	0.94 ± 0.02	8.40 ± 0.04	0.89(0.89)*	4.13 ± 0.04
	105	0.79 ± 0.01	1.01 ± 0.03	8.36 ± 0.05	1.13(1.04)*	4.01 ± 0.06
	120	0.78 ± 0.01	0.93 ± 0.03	8.41 ± 0.05	1.18(1.13)*	4.06 ± 0.06
	141	0.81 ± 0.01	•••	8.31 ± 0.06	(1.34)*	•••
	176	0.81 ± 0.02	•••	7.90 ± 0.10	•••	4.16 ± 0.06
I_H^H	90	0.77 ± 0.01	•••	7.58 ± 0.03	•••	4.14 ± 0.03
(T=4.5 °C) I_H^V	45	0.74 ± 0.01	0.60 ± 0.02	5.40 ± 0.04	0.38(0.43)*	2.47 ± 0.05
	60	0.83 ± 0.02	0.74 ± 0.01	5.67 ± 0.04	0.56(0.55)*	2.51 ± 0.04
	75	0.85 ± 0.02	0.80 ± 0.02	5.90 ± 0.05	0.67(0.71)*	2.59 ± 0.05
(T=4.5 °C) I_H^V	90	0.81 ± 0.01	0.83 ± 0.03	5.98 ± 0.05	0.82(0.87)*	2.60 ± 0.05
	105	0.76 ± 0.01	0.82 ± 0.03	5.98 ± 0.04	0.92(0.96)*	2.60 ± 0.06
	120	0.76 ± 0.01	0.60 ± 0.04	5.85 ± 0.04	0.71(1.15)*	2.68 ± 0.07
Aniline						
(T=20.0 °C) I_H^V	45	0.91 ± 0.01	0.87 ± 0.03	11.57 ± 0.09	0.50 ± 0.05	6.62 ± 0.09
	60	0.91 ± 0.02	1.03 ± 0.03	11.55 ± 0.15	0.72 ± 0.06	6.51 ± 0.18
	75	0.91 ± 0.01	1.11 ± 0.04	11.67 ± 0.08	0.93 ± 0.07	6.52 ± 0.10
	90	0.94 ± 0.01	1.20 ± 0.04	11.81 ± 0.12	1.14(1.05)*	6.67 ± 0.14
	105	0.91 ± 0.01	1.24 ± 0.10	11.95 ± 0.20	1.33(1.16)*	6.59 ± 0.24
	120	0.91 ± 0.01	1.25 ± 0.02	11.75 ± 0.10	1.57(1.26)*	6.40 ± 0.20
I_H^H	90	0.91 ± 0.01	•••	9.99 ± 0.14	•••	6.73 ± 0.26
(T=3.5 °C) I_H^V	45	0.82 ± 0.01	0.75 ± 0.03	6.97 ± 0.05	0.50(0.50)*	3.32 ± 0.04
	60	0.82 ± 0.01	0.92 ± 0.02	7.26 ± 0.07	0.74(0.73)*	3.39 ± 0.10
	75	0.85 ± 0.02	1.04 ± 0.03	7.50 ± 0.07	0.96(0.82)*	3.44 ± 0.07
	90	0.82 ± 0.01	1.07 ± 0.03	7.44 ± 0.12	1.10(1.04)*	3.36 ± 0.10
	105	0.82 ± 0.01	1.05 ± 0.03	7.97 ± 0.10	1.19(1.30)*	3.70 ± 0.11

is observed in the I_H^V spectrum, a Brillouin doublet would be expected in the I_H^H spectrum.

An unambiguous identification of the weak doublet shown in Figs. 2(c) and 7 is not trivial. For example, the observed spectrum may be complicated by the polarized Brillouin doublet which appears for all angles $\theta \neq 90°$. Thus near $\theta = 90°$, the observed peak intensity of the doublet in the I_H^H spectrum is expected to be approximated by

$$I_H^H(\theta) = I_H^H(90°) + \cos^2(\theta) I_V^V . \quad (13)$$

Also, the predicted magnitude and breadth of the depolarized Brillouin doublet are very sensitive to the instrumental line profile, as shown in Fig. 8. For large instrumental breadths ($\Delta\nu_I > 1.5$ GHz) the doublet profile broadens to such an extent that it merges with the main component; this is no doubt the reason that the depolarized Brillouin doublet had not been detected in earlier experiments.

An experimental test of Eq. (13) was carried out for scattering near 90° in nitrobenzene, and some of the spectra are shown in Fig. 9. Note

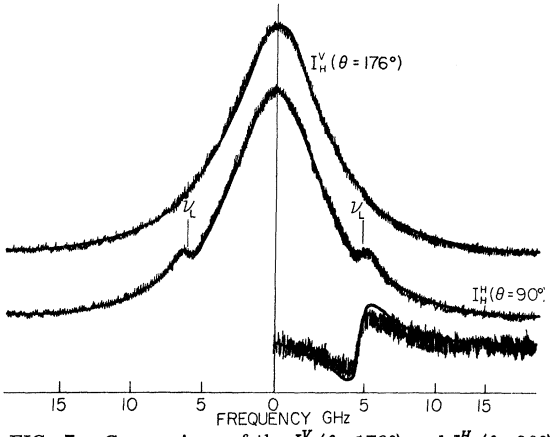

FIG. 7. Comparison of the $I_H^V(\theta = 176°)$ and $I_H^H(\theta = 90°)$ spectra of quinoline. The difference between the two spectra is also shown magnified five times. The best fit to the Rytov theory is given by the solid lines.

that all three spectra exhibit Brillouin doublets: In addition, those at 75° and 100° exhibit a sharp Rayleigh line superimposed on the broader central

TABLE II. Shear-wave frequencies and linewidths from I_H^V spectra at various scattering angles and temperatures (see Ref. 12). The liquid referred to is quinoline.

Temp. (°C)	Scattering angle θ (deg)	Instrumental linewidth $\Delta\nu_I$ (GHz)	Observed peak shift ν_S (GHz)	Observed linewidth $2\Gamma_S$ (GHz)	Shear-wave frequency ν_T (GHz)	Linewidth Γ (GHz)
−20.2	60	0.68 ± 0.02	0.37 ± 0.02	2.77 ± 0.05	0.59* ± 0.05	0.88 ± 0.02
−21.0	90	0.68 ± 0.02	•••	2.55 ± 0.09	0.90* ± 0.05	•••
−13.8	60	0.70 ± 0.02	0.55 ± 0.02	3.27 ± 0.05	0.50* ± 0.04	1.19 ± 0.02
−13.5	90	0.81 ± 0.02	•••	3.60 ± 0.05	0.81* ± 0.06	•••
−8.5	60	0.80 ± 0.02	0.63 ± 0.02	3.82 ± 0.05	0.54* ± 0.04	1.43 ± 0.05
−8.8	90	0.80 ± 0.02	0.61 ± 0.03	4.14 ± 0.05	0.78* ± 0.07	1.63 ± 0.05
−7.0	90	0.76 ± 0.02	0.69 ± 0.04	4.33 ± 0.04	0.64 ± 0.04	2.04 ± 0.05
−1.2	60	0.74 ± 0.02	0.69 ± 0.02	4.76 ± 0.05	0.63* ± 0.05	2.01 ± 0.04
−1.2	90	0.74 ± 0.02	0.79 ± 0.03	5.13 ± 0.04	0.82* ± 0.05	2.12 ± 0.06
−0.3	90	0.76 ± 0.02	0.79 ± 0.02	5.04 ± 0.03	0.76 ± 0.04	2.58 ± 0.06
8.5	90	0.78 ± 0.02	0.84 ± 0.02	5.43 ± 0.08	0.82 ± 0.05	2.92 ± 0.08
11.5	90	0.77 ± 0.02	0.88 ± 0.01	5.65 ± 0.05	0.87 ± 0.03	3.16 ± 0.09
15.0	60	0.76 ± 0.02	0.78 ± 0.02	7.12 ± 0.07	0.56* ± 0.04	3.42 ± 0.06
15.0	90	0.76 ± 0.02	0.92 ± 0.01	7.48 ± 0.07	0.92* ± 0.04	3.54 ± 0.07
16.9	90	0.78 ± 0.02	0.92 ± 0.03	6.13 ± 0.04	0.89 ± 0.04	3.73 ± 0.10
21.8	90	0.77 ± 0.02	0.95 ± 0.03	6.43 ± 0.03	0.92 ± 0.05	4.09 ± 0.12
22.2	90	0.78 ± 0.02	0.93 ± 0.01	6.40 ± 0.04	0.89 ± 0.02	4.14 ± 0.07
27.6	90	0.77 ± 0.02	0.96 ± 0.02	6.84 ± 0.04	0.92 ± 0.03	4.99 ± 0.15
30.1	90	0.78 ± 0.02	0.99 ± 0.02	6.91 ± 0.04	0.94 ± 0.03	5.06 ± 0.15
30.5	60	0.78 ± 0.02	0.86 ± 0.02	9.77 ± 0.12	0.59 ± 0.05	5.16 ± 0.07
30.5	90	0.81 ± 0.02	1.00 ± 0.01	9.96 ± 0.04	0.91* ± 0.04	5.19 ± 0.04
34.4	90	0.78 ± 0.02	0.96 ± 0.02	6.90 ± 0.07	0.90 ± 0.04	5.13 ± 0.25
39.8	60	0.78 ± 0.02	0.85 ± 0.02	11.38 ± 0.09	0.53 ± 0.05	6.50 ± 0.12
39.8	90	0.81 ± 0.02	1.01 ± 0.02	11.55 ± 0.08	0.91* ± 0.04	6.49 ± 0.10
40.3	90	0.79 ± 0.02	1.00 ± 0.03	7.38 ± 0.09	0.91 ± 0.05	6.75 ± 0.50
41.8	90	0.78 ± 0.02	1.02 ± 0.05	7.39 ± 0.07	0.93 ± 0.09	6.74 ± 0.53
49.5	90	0.77 ± 0.02	1.01 ± 0.03	12.63 ± 0.10	0.88* ± 0.05	7.48 ± 0.13
61.0	90	0.76 ± 0.02	1.04 ± 0.05	14.48 ± 0.11	0.92 ± 0.07	9.66 ± 0.19
72.0	90	0.76 ± 0.02	1.05 ± 0.13	16.00 ± 0.20	0.90 ± 0.08	12.10 ± 0.50

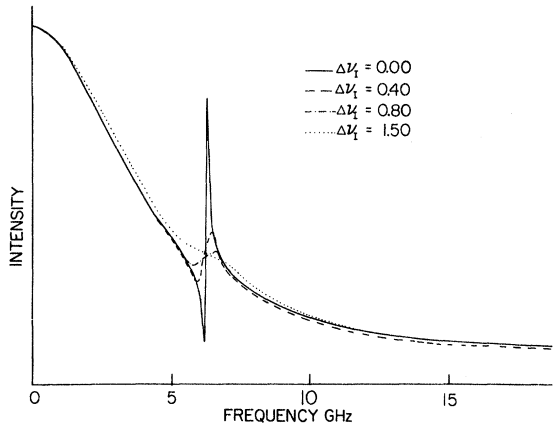

FIG. 8. Calculated I_H^H spectra for various instrumental linewidths $\Delta\nu_I$. (Values of 0.90, 6.2, and 4.14 GHz were assumed for ν_T, ν_L, and Γ, respectively.)

component, but the spectrum at 90° scattering shows no sign of such a Rayleigh line. This observation alone is sufficient proof that the I_H^H doublet at 90° is real and is not a result of spurious scattering. Further proof is found in the graph of peak intensities of the Brillouin components vs scattering angle, in Fig. 10, whose intercept on the ordinate axis is evidence of considerable depolarized scattering at $\theta = 90°$. An upper limit to spurious scattering was established from experiments with ethyl ether. Its depolarized spectrum is very weak and without structure (within the bandwidth of the interferometer). A weak Brillouin doublet observed in the I_H^H spectrum and believed to arise from incomplete polarization of the incident light was found to be only a factor of 10^{-4} of the polarized Brillouin doublet in the I_V^V spectrum. This was also taken to represent an upper limit to the depolarized Brillouin intensity due to spurious causes in the nitrobenzene experiments and is shown by the cross-hatched section in Fig. 10.

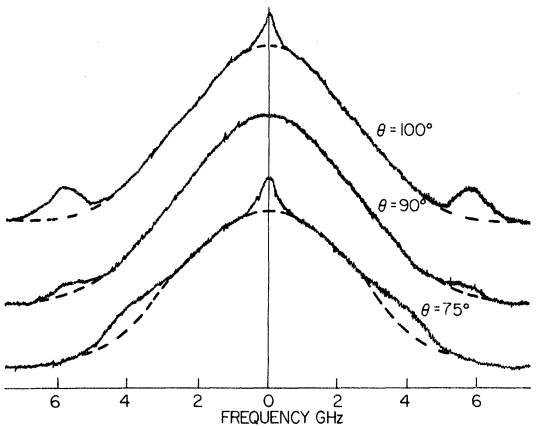

FIG. 9. I_H^H spectra of nitrobenzene for $\theta = 75°$, 90°, 100°.

The contribution which remains proves that the Brillouin doublet in the I_H^H spectrum is real and does not arise from experimental defects.

At the bottom of Fig. 7 is shown the difference of the Lorentzian profile observed in the I_H^V (180°) spectrum and the I_H^H (90°) spectrum (after normalization to the same integrated intensities) magnified by a factor of 5. The resulting curve is in good agreement with that predicted from Eqs. (10) and (11). This result also reveals the appreciable departure of the central component of the I_H^H (90°) spectrum from a Lorentzian profile in the region of the depolarized doublet. The peak of the depolarized Brillouin component occurs at a higher frequency than the Brillouin peak observed at 90° in the I_V^V spectrum of quinoline. The measured difference is ~ 400 MHz, while the predicted difference of $2\nu_T^2/3\nu_L$ has a value of ~ 100 MHz for quinoline. This shift of the observed depolarized peak to even higher frequencies than predicted theoretically is caused by the effect of the instrumental linewidth on the I_H^H spectrum (Fig. 8).

The degree to which the central component of the I_H^H spectrum has a Lorentzian profile in the wings of the line was also examined. For this study, the I_H^H spectrum of anisaldehyde near its freezing point was chosen, since its linewidth was only 1.5 GHz and the line profile could be examined out to 20Γ (with a 37-GHz spectral free range for the interferometer). The observed and calculated spectra agree very well except in the limited region near ν_L (as discussed above).

The linewidth $\Gamma = (2\pi\tau)^{-1}$ of the central component in the I_H^H spectrum was evaluated in the same manner as that described for the doublet in the I_H^V

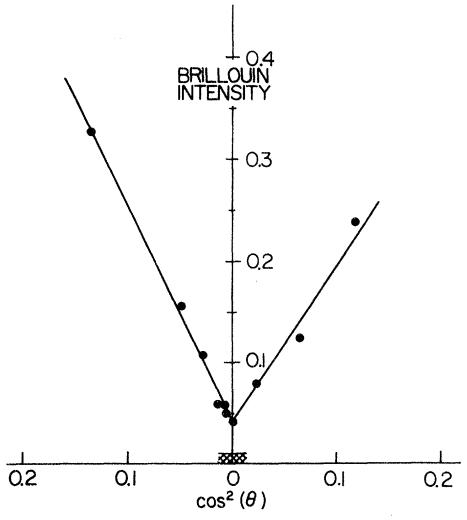

FIG. 10. Measured intensity of Brillouin component of nitrobenzene in the I_H^H spectra plotted against $\cos^2\theta$. The cross-hatched level is twice the Brillouin intensity due to parasitic light.

TABLE III. Linewidths of I_H^H components (for $\theta = 90°$) at various temperatures for the liquid quinoline (see Ref. 12).

Temp. (°C)	Instrumental linewidth $\Delta\nu_I$ (GHz)	Observed linewidth $2\Gamma_S$ (GHz)	Brillouin shift ν_L (GHz)	Linewidth Γ (GHz)
−21.6	0.68 ± 0.02	1.49 ± 0.03	7.4	0.56 ± 0.03
−20.0	0.83 ± 0.02	1.70 ± 0.03	7.4	0.61 ± 0.02
−14.6	0.94 ± 0.02	2.35 ± 0.04	7.2	0.94 ± 0.04
−13.8	0.81 ± 0.02	2.48 ± 0.05	7.2	1.06 ± 0.04
−9.0	0.87 ± 0.02	2.91 ± 0.06	7.1	1.28 ± 0.04
−8.9	0.80 ± 0.02	2.84 ± 0.06	7.1	1.27 ± 0.03
0.0	0.83 ± 0.02	4.29 ± 0.06	6.9	2.07 ± 0.04
4.5	0.81 ± 0.02	5.06 ± 0.06	6.7	2.52 ± 0.04
4.7	0.84 ± 0.02	5.04 ± 0.07	6.7	2.50 ± 0.05
15.0	0.76 ± 0.02	6.57 ± 0.07	6.5	3.46 ± 0.05
15.2	0.81 ± 0.02	6.69 ± 0.07	6.5	3.52 ± 0.05
22.3	0.77 ± 0.02	7.58 ± 0.04	6.2	4.14 ± 0.02
25.0	0.86 ± 0.02	8.10 ± 0.08	6.2	4.48 ± 0.07
30.5	0.81 ± 0.02	8.93 ± 0.10	6.1	5.17 ± 0.08
35.0	0.93 ± 0.02	9.73 ± 0.07	6.0	5.95 ± 0.13
39.8	0.81 ± 0.02	10.01 ± 0.10	5.9	6.33 ± 0.31
48.0	0.96 ± 0.02	12.00 ± 0.13	5.7	7.04 ± 0.21
49.5	0.77 ± 0.02	11.78 ± 0.19	5.7	7.44 ± 0.59
72.0	0.76 ± 0.02	16.10 ± 0.33	5.4	11.97 ± 0.85

spectrum. That is, a trial value of Γ was varied until computer-generated spectra (corrected for the instrumental profile) and the observed spectra produced the same value of Γ_s, the observed linewidth. Values of ν_L and ν_T necessary for these calculations were measured from the I_V^V and I_H^V spectra, respectively. For example, for quinoline at 22.4 °C and a scattering angle of 90°, $\nu_L = 6.2$ GHz and $\nu_T = 0.92$ GHz. A value of $\Gamma = 4.14 \pm 0.03$ GHz was determined, in agreement with the value 4.16 ± 0.05 GHz deduced from an analysis of the I_H^V spectrum. These yield values of the relaxation time $\tau = (3.85 \pm 0.03) \times 10^{-11}$ and $(3.83 \pm 0.05) \times 10^{-11}$ sec, respectively. An examination of Rytov's theory reveals that the width of the I_H^H component is determined essentially by τ_X, the anisotropy relaxation time, while the width of the doublet in the I_H^V spectrum is mainly dependent on τ_μ, the shear relaxation time. The present results show that in quinoline $\tau_X = \tau_\mu$. Values of the linewidth Γ derived from I_H^H spectra are given in Tables I, III, and IV.[12]

C. Temperature Dependence of I_H^V and I_H^H Spectra

The behavior of the depolarized spectra at various temperatures was also investigated and the effects of temperature on linewidth, shear-wave frequency, and total scattering intensity were noted. Again, the most detailed experiments were carried out with quinoline, aniline, and nitrobenzene, and the measurements are given in Tables II and III.[12] The measurements for other liquids investigated are presented in Table IV.[12]

The most prominent change in the spectra is the rapid increase in linewidth Γ with increasing temperature. This behavior is shown in the graphs of Fig. 11. The largest temperature range covered was that for liquid quinoline, from its freezing point of −21 to 72 °C, and in this range the change in Γ is a factor of ~20. Over most of the temperature ranges studied, the values of Γ obtained from the I_H^V and I_H^H spectra are in good agreement (except near the freezing points of aniline and quinoline).

As already discussed in Sec. IV A, measurements of the shear-wave frequency ν_T at various scattering angles and at two different temperatures obey Brillouin's relation $\nu_T \propto \sin\frac{1}{2}\theta$ as shown in Fig. 6. In fact, the values of ν_T for both temperatures fall on the same straight line, within the accuracy of the measurements, indicating that ν_T is not strongly dependent on temperature. Measurements of ν_T vs temperature are shown in Fig. 12. For nitrobenzene, ν_T (at $\theta = 90°$) remains con-

TABLE IV. Shear-wave frequency shifts and linewidths of I_H^V and I_H^H spectra (for $\theta = 90°$) at various temperatures (see Ref. 12).

	T (°C)	ν_T (GHz)	$\Gamma(I_H^V)$ (GHz)	$\Gamma(I_H^H)$ (GHz)
m-nitrotoluene	20.0	0.40 ± 0.04	2.82 ± 0.06	2.81 ± 0.06
o-nitroanisole	20.5	0.34 ± 0.02	1.85 ± 0.03	•••
Bromobenzene	4.0	0.64 ± 0.16	10.13 ± 0.28	9.75 ± 0.4
Chlorobenzene	2.0	0.68 ± 0.15	13.84 ± 0.70	13.91 ± 0.8
o-dichlorobenzene	22.4	0.55 ± 0.05	8.65 ± 0.17	8.71 ± 0.15
m-dichlorobenzene	22.4	0.35 ± 0.05	9.18 ± 0.14	9.25 ± 0.20
p-dichlorobenzene	58.0	0.40 ± 0.05	•••	12.20 ± 0.40
1, 3, 5 trichlorobenzene	66.0	0.30 ± 0.05	8.44 ± 0.24	8.52 ± 0.07
1, 2, 4 trichlorobenzene	22.4	0.33 ± 0.03	3.30 ± 0.10	3.28 ± 0.04
Hexafluorobenzene	22.2	0.46 ± 0.04	11.50 ± 0.40	11.60 ± 0.30
Benzonitrile	22.5	0.51 ± 0.04	8.21 ± 0.15	8.29 ± 0.15
Diphenyl methane	27.0	0.32 ± 0.06	3.31 ± 0.37	•••
Dibromo ethane	14.0	0.25 ± 0.05	6.73 ± 0.43	•••
Anisaldehyde	22.5	0.33 ± 0.04*	•••	1.05 ± 0.05
Benzyl benzoate	22.5	0.25 ± 0.06*	•••	0.64 ± 0.03
α-bromonaphthalene	40.5	0.38 ± 0.02	2.87 ± 0.04	2.88 ± 0.04
α-chloronaphthalene	22.5	0.38 ± 0.03	2.38 ± 0.08	2.30 ± 0.04
Tetralin	21.7	0.51 ± 0.05	5.04 ± 0.16	4.95 ± 0.06
Decalin	−1.5	0.73 ± 0.12	3.26 ± 0.13	•••

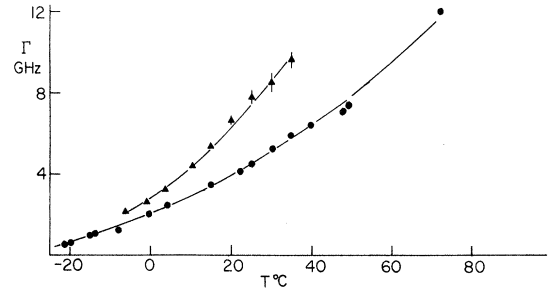

FIG. 11. Graphs of spectral breadth Γ plotted against temperature, for aniline (▲) and quinoline (●).

stant over the temperature range 5–50 °C; for aniline, ν_T is independent of temperature at $\theta = 45°$ and 60°, but decreases by ~ 10% below 0 °C at $\theta = 90°$; similarly, while ν_T is independent of temperature over most of the range studied for quinoline, it decreases by ~ 30% below 10 °C at $\theta = 90°$ and below − 10 °C at $\theta = 60°$. For both aniline and quinoline these "anomalous" regions are characterized by decreasing ν_T with decreasing temperature, larger Γ from the I_H^V spectra than from the I_H^H spectra, and deterioration of the good agreement found at higher temperatures between the observed and computed profiles for the I_H^V spectra.

The above observations cannot be resolved within the framework of the present theory. Neither spurious laser scattering nor a two-relaxation-time ($\tau_\mu \neq \tau_\chi$) formalism provide a satisfactory explanation for the anomaly noted in the shear-wave frequency. However, if ν_T from the simple analysis is plotted against Γ, as in Fig. 13, then a systematic dispersion occurs when $3\nu_T > \Gamma$ (or $\omega_T \tau > 0.3$); that is, the assumptions made in the theory are apparently valid as long as the shear waves are heavily damped. Discrepancies which arise when $\omega_T^2 \tau^2$ becomes significant relative to unity imply that the single-relaxation-time form assumed for μ is inadequate.[13]

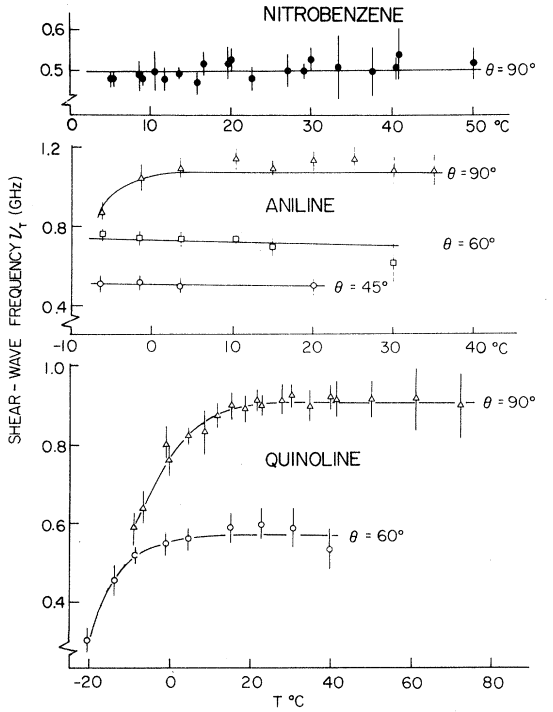

FIG. 12. Variation of shear-wave frequency with temperature for nitrobenzene, aniline, and quinoline at various scattering angles.

TABLE V. Total depolarized intensity[a] and percentage contribution of the shear-wave spectrum for various liquids.

	Total intensity	Percent shear		Total intensity	Percent shear
Benzene	1.0	···	1,2,4 trichlorobenzene	9.3	76
Aniline	1.3	34	Hexafluorobenzene	1.0	74
Nitrobenzene	4.7	74	Benzonitrile	4.3	48
m-nitrotoluene	5.0	50	Diphenyl methane	0.9	45
o-nitroanisole	6.0	46	Dibromo ethane	1.4	74
Bromobenzene	1.8	48	Quinoline	6.0	35
Chlorobenzene	1.9	38	α-bromonaphthalene	6.0	35
o-dichlorobenzene	2.8	67	α-chloronaphthalene	6.9	55
m-dichlorobenzene	2.8	74	Tetralin	1.2	61
p-dichlorobenzene	3.4	70	Decalin	0.2	14
1,3,5 trichlorobenzene	4.1	49			

[a]The total depolarized intensity is normalized to unity for benzene.

D. Broad Depolarized Background

The I_H^V and I_H^H spectra described above do not account for all of the observed depolarized scattering. There is another much broader component underlying these spectra which appears as a background of constant intensity in our spectra. Its appearance as a straight-line background occurs because of the small bandwidth of the interferometer and the overlap of many successive orders. This broad

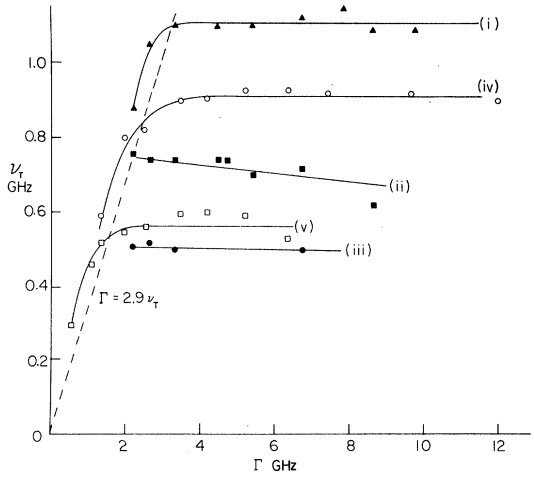

FIG. 13. Graphs of shear-wave frequency ν_T plotted against linewidth Γ for aniline at $\theta = 90°$ (i), 60° (ii), and 45° (iii), and for quinoline, $\theta = 90°$ (iv) and 60°(v). The dashed line through the origin represents values of $\Gamma \sim 3\nu_T$.

component, often called the "Rayleigh wing," has been the subject of numerous investigations in the past, and, more recently, excitation with laser sources has led to accurate linewidth measurements for many liquids.[14] Typical linewidths of the broad components are at least a factor of 10 larger than those of the main components of the I_H^V and I_H^H spectra.

Our main interest was in the measurement of the relative intensities of these broad components and of the percentage contribution of the shear-wave components for the various liquids investigated. The observed relative intensity of the broad background was found to depend on several experimental factors such as reflectivity of the interferometer plates, sensitivity of the photomultiplier tube, and for some liquids the purity of the sample. Intensity measurements were made with insertion of a 30-Å bandpass filter after the sample cell in order to reduce contributions arising from Raman vibrational bands and fluorescence.

The total integrated intensities of depolarized scattering normalized to a value of 1.0 for benzene were determined to an accuracy of ±15% and are listed in Table V. Also listed are the percentage contributions of the shear-wave components to the total depolarized intensities. For the liquids studied these ratios appear to fall in two ranges, ~70 and ~40%. The contributions of the I_H^V shear-wave components to the total integrated intensities were found to be independent of temperature (to within ±5%) for all the liquids studied. However, the total integrated intensities for three of the liquids, nitrobenzene, *m*-nitrotoluene, and 1, 2, 4 trichlorobenzene, were found to vary with temperature (Fig. 14), while for most of the liquids the total intensities remained essentially constant over the small temperature ranges investigated.

V. SUMMARY OF OBSERVATIONS AND OF DERIVED QUANTITIES

A list of the 27 molecular liquids investigated is given in Table VI. Well-resolved shear-wave doublets were observed in the I_H^V spectra of the first 20 liquids on this list. While no doublet structure was observed in the spectra of anisalde-

TABLE VI. Properties[a] of the liquids investigated.

	Freezing point (0 °C)	Density ρ_{20} (g/cm^3)	Refractive index n	Dipole moment (D)[b]	Viscosity η_{20} (cp)
Aniline	−6	1.02	1.58	1.6	4.4
Nitrobenzene	6	1.20	1.55	4.0	2.0
m-nitrotoluene	15	1.16	1.54	4.2	2.3
o-nitroanisole	10	1.25	1.56	4.8	8.6
Bromobenzene	−31	1.50	1.55	1.6	1.1
Chlorobenzene	−45	1.11	1.53	1.6	0.8
o-dichlorobenzene	−18	1.31	1.55	2.3	1.9
m-dichlorobenzene	−25	1.29	1.54	1.7	1.8
p-dichlorobenzene	53	1.25[c]	1.52	0.0	0.8
1, 3, 5 trichlorobenzene	63	1.38[d]	1.56	0.0	0.9
1, 2, 4 trichlorobenzene	17	1.47	1.56	1.3	2.0
Hexafluorobenzene	5	1.62	1.49	0.0	0.9
Benzonitrile	−13	1.01	1.52	3.9	2.0
Anisaldehyde	3	1.12	1.57	3.5	4.2
Diphenyl methane	26	1.00	1.57	0.2	3.0
Dibromo ethane	10	2.18	1.54	1.5	1.7
Benzyl benzoate	17	1.16	1.56	2.0	8.3
Quinoline	−20	1.10	1.62	2.3	4.0
α-bromonaphthalene	3	1.49	1.65	1.6	10.5
α-chloronaphthalene	<0	1.19	1.63	1.5	7.2
Tetralin	−30	0.97	1.54	0.5	2.3
Decalin	−35	0.88	1.47	0.0	2.6
Benzene	5	0.88	1.49	0.0	0.7
Cyclohexane	6	0.78	1.42	0.0	1.0
Nitromethane	−29	1.13	1.38	3.5	0.6
Isobutanol	−90	0.81	1.39	1.6	4.6
Carbon tetrachloride	−23	1.59	1.45	0.0	1.0

[a]Values from *Handbook of Chemistry and Physics* (The Chemical Rubber Co., Cleveland, Ohio, 1963), 44th ed.; *International Critical Tables of Numerical Data, Physics, Chemistry and Technology* (McGraw-Hill, New York, 1928); J. Timmermans, *Physico-Chemical Constants of Pure Organic Compounds* (Elsevier, New York, 1965).

[b]A. L. McLellan, *Tables of Experimental Dipole Moments* (W. H. Freeman, San Francisco, 1963).

[c]At 55 °C.

[d]At 63 °C.

hyde and benzyl benzoate, the observed linewidths in the I_H^V spectra were ~ 20% larger than in the I_H^H spectra and this was considered as evidence of shear-wave spectra. The depolarized spectra I_H^V and I_H^H of the last five liquids listed in Table VI exhibited a constant intensity, without any structure within the 15-GHz bandwidth of the interferometer.

Measurements of the doublet separations and linewidths and the deduced values of ν_T and Γ are presented in Tables I–IV. Values of the shear-wave frequencies ν_T for scattering at 90° are summarized in Table VII along with the values of the transverse sound velocities V_T derived from $V_T = \nu_T / 2nk_0 \sin\frac{1}{2}\theta$. The values of ν_T ranged from a lower limit of ~ 0.25 GHz in several liquids to a maximum of 1.05 GHz for aniline. The angular and temperature dependence of ν_T agreed well with the predictions of Rytov's theory: The relation $\nu_T \propto \sin\frac{1}{2}\theta$ was confirmed indicating a propagating mode; and ν_T was found to be essentially independent of temperature. A small dispersion in ν_T was observed for quinoline and aniline, when $3\nu_T > \Gamma$, and attributed to an inadequacy of the single relaxation time assumed in Rytov's theory.

The spectral breadths Γ deduced from the I_H^V and I_H^H spectra were equal to within the experimental uncertainty for each liquid. Values of the relaxation time $\tau = (2\pi\Gamma)^{-1}$ are listed in Table VII and are seen to range from 1.3 to 25×10^{-11} sec. Linewidths Γ were found to increase rapidly and non-

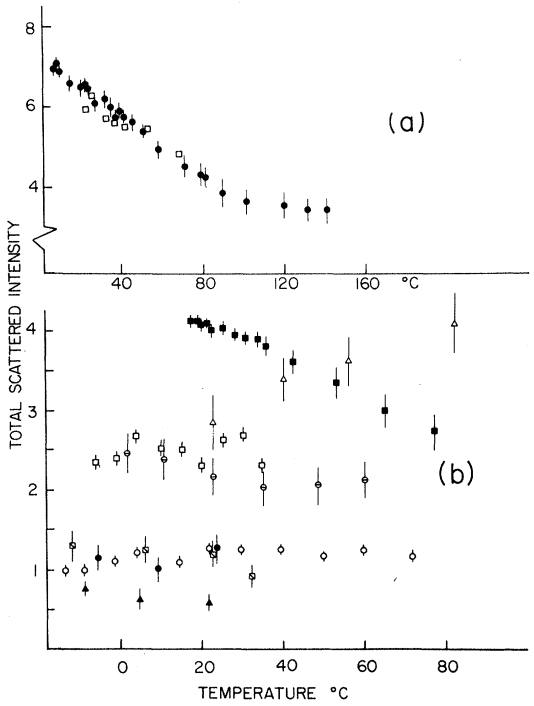

FIG. 14. Measured relative values of total scattered intensity plotted against temperature. (a) Nitrobenzene; • this experiment, □ Ref. 21. (b) Aniline (□); quinoline (○); *m*-nitrotoluene (■); 1,2,4 trichlorobenzene (△); α-chloronaphthalene (⊖); benzonitrile (⧅); tetralin (▲); and *m*-dichlorobenzene (●).

TABLE VII. Summary of measured and derived quantities from depolarized spectra.

	Shear freq. ν_T (GHz)	Shear velocity V_T (m/sec)	Relax. time τ (10^{-11} sec)	Decay length (Å)	Shear modulus μ_∞ (10^8 dyn/cm^2)	$\frac{\mu_\infty \tau}{\eta}$
Aniline	1.05	289	2.4[a]	70	8.5 ± 0.8	0.5
Nitrobenzene	0.50	144	3.9[b]	56	2.5 ± 0.2	0.5
m-nitrotoluene	0.42	122	5.7[a]	70	1.7 ± 0.3	0.4
o-nitroanisole	0.37	106	8.6[a]	91	1.4 ± 0.5	0.2
Bromobenzene	0.64	180	1.6[c]	29	5.1 ± 2.0	0.6
Chlorobenzene	0.68	200	1.2[d]	24	4.4 ± 2.0	0.5
o-dichlorobenzene	0.55	159	3.4[b]	54	3.3 ± 1.0	0.5
m-dichlorobenzene	0.35	102	1.7[b]	17	1.3 ± 0.3	0.2
p-dichlorobenzene	0.40	117	1.3[e]	15	1.7 ± 0.5	0.3
1,3,5 trichlorobenzene	0.30	87	1.9[f]	17	1.1 ± 0.3	0.2
1,2,4 trichlorobenzene	0.31	89	4.9[b]	43	1.2 ± 0.3	0.3
Hexafluorobenzene	0.49	160	1.4[b]	22	4.0 ± 1.0	0.6
Benzonitrile	0.52	150	1.9[b]	28	2.3 ± 0.5	0.3
Anisaldehyde	0.33	94	15.2[b]	140	1.0 ± 0.5	0.4
Diphenyl methane	0.25	91	5.9[b]	54	0.8 ± 0.3	0.2
Dibromo ethane	0.25	63	2.0[a]	12	0.9 ± 0.5	0.1
Benzyl benzoate	0.25	72	25.0[b]	180	0.6 ± 0.3	0.2
Quinoline	0.90	245	3.8[b]	93	6.6 ± 0.5	0.7
α-bromonaphthalene	0.40	105	10.5[a]	110	1.8 ± 0.4	0.4
α-chloronaphthalene	0.39	104	6.9[b]	72	1.2 ± 0.2	0.3
Tetralin	0.52	154	3.2[b]	49	2.3 ± 0.5	0.4
Decalin	0.73	222	3.0[b]	67	4.3 ± 1.6	0.5

[a]20.0 °C. [b]22.4 °C. [c]4.0 °C. [d]3.0 °C. [e]58.0 °C. [f]66.0 °C.

linearly with increasing temperature; the widths for quinoline were observed to change from a minimum of 0.55 GHz at $-21\,^{\circ}$C to a maximum of 12 GHz at $72\,^{\circ}$C. Finally, a weak depolarized doublet was observed in the I_H^H spectrum and identified with the doublet at $\nu_T \pm 2\nu_T^2/3\nu_L$ predicted by Eq. (11). These observations are all in agreement with the Rytov theory.

The distances over which the shear waves propagate were estimated from the product of velocity and relaxation time, and are given in Table VII. Values ranging from 10 to 200 Å were found for the various liquids near $20\,^{\circ}$C. These propagation lengths are extremely short compared to the wavelengths of the shear waves themselves, approximately 3000 Å, and to the propagation lengths of longitudinal waves, $\sim 10^5$ Å. Even at the lowest temperatures the propagation lengths for the shear waves in aniline and quinoline are at most only about one-tenth of their wavelengths. Thus the collective motions associated with shear waves in these liquids appear to involve only from tens to hundreds of molecules.

Values of the high-frequency shear modulus μ_∞ were calculated from the relation $\mu_\infty = \rho V_T^2$ (with values of the density ρ listed in Table VI), and are included in Table VII. The shear moduli were found to be generally two orders of magnitude smaller than the bulk moduli for these liquids and varied from 0.6×10^8 dyn/cm^2 in benzyl benzoate to 8.5×10^8 dyn/cm^2 in aniline. Also, since values of ν_T and therefore V_T were observed to be independent of temperature, we conclude that the values of μ_∞ are constant within the experimental uncertainty.

According to Rytov's theory, the shear modulus μ_∞ is related to the relaxation time τ by $\mu_\infty\tau/\eta = 1$ as given in Eqs. (4) and (5). Values of this product for the liquids investigated are listed in Table VII. All of the values are less than unity, and range from 0.1 to 0.7. This result contradicts the assumption made by Rytov and by Leontovich for the dependence of μ_∞ on τ.

VI. FACTORS DETERMINING EXISTENCE AND OBSERVATION OF SHEAR-WAVE SPECTRA

The dipole moment and viscosity were considered as possible properties related to the existence of shear-wave spectra. Thus the liquids chosen for investigation included as large a range of values as possible (Table VI). Depolarized doublets were observed for liquids composed of molecules with dipole moments ranging from 0 (hexafluorobenzene) to 4.8 D (*o*-nitroanisole). The lowest value of the viscosity at which a doublet was detected is 0.82 cp (*p*-dichlorobenzene) and the viscosities of the samples which did not exhibit shear-wave spectra were all of this order or greater.

The relation of molecular structure and local liquid structure to the existence of shear-wave spectra was also explored. Most of the liquids examined were composed of planar molecules and, with the exception of benzene, all exhibited depolarized doublets. However, the liquids dibromoethane, diphenylmethane, and benzyl benzoate composed of nonplanar molecules also exhibited depolarized doublets. Furthermore, for the planar molecules, the symmetry of the polarizability in the molecular plane is not a factor, as shear-wave spectra were observed for both hexafluorobenzene and 1, 3, 5 trichlorobenzene. The broad depolarized spectrum of liquid carbon tetrachloride (spherical molecules) showed no doublet and is thought to arise from induced anisotropy caused by the strong interactions of neighboring molecules.[15]

Techniques have been developed[16] by which electron and x-ray diffraction patterns of liquids consisting of planar molecules can be interpreted in terms of either a T or a parallel-plane local liquid structure. In the former, the planes of adjacent molecules are arranged in a T configuration, and in the latter, adjacent molecular planes are parallel to one another. A local T configuration was derived for benzene, aniline, decalin, and tetralin, while nitrobenzene, *m*-nitrotoluene, quinoline, nitromethane, *p*-dichlorobenzene 1, 3, 5 trichlorobenzene, and α-bromonaphthalene stack locally in parallel planes. Both configurations contain liquids which do and do not exhibit depolarized doublets. Thus the depolarized shear-wave spectra are not dependent on the local liquid structure (and conversely they cannot provide information about the local structure in liquids). In conclusion, it is apparent that one of the physical properties required for the existence of a depolarized doublet in the spectrum of scattered light is that the liquid be composed of molecules with anisotropic polarizability.

The effects of the relaxation time and the instrumental resolution were found to be of prime importance on the detectability of shear-wave doublets. For the five liquids for which no doublets were observed in the depolarized spectra, the intensity of depolarized scattering was constant over the frequency bandwidth of the interferometer, ~ 15 GHz. Thus it is inferred that if a contribution due to shear waves were present, the associated relaxation time must be shorter than 10^{-11} sec. For such short relaxation times, an estimate of the detectability of a shear-wave doublet may be made from Eq. (10). In the limit $\omega_T\tau \ll 1$, the integrated area of the intensity minimum of the I_H^V component depends on the product $\omega^2\tau^2$. An additional factor $\omega_T/\Delta\nu_I$ takes into account the effect of the instrumental width. Therefore, the resolution of the doublet predicted by Eq. (10) is critical-

ly dependent on the shear-wave frequency ($\propto \omega^3$), the relaxation time ($\propto \tau^2$), and to a lesser extent on the instrumental width [$\propto(1/\Delta\nu_I)$]. The small values of τ are thus considered to be responsible for our not observing depolarized doublets in the spectra of benzene, cyclohexane, nitromethane, and isobutanol.

In summary, it is expected that the depolarized spectrum of any liquid composed of anisotropic molecules would contain a doublet due to scattering from shear waves. However, the observation of such a doublet is limited by the magnitude of the relaxation time τ and by the instrumental resolution and available signal-to-noise level.

VII. COMPARISON OF SHEAR MODULI AND RELAXATION TIMES WITH VALUES FROM OTHER EXPERIMENTS

A. Shear Modulus μ_∞

As already mentioned (Sec. III), shear moduli of rigidity have been measured[3] for very viscous liquids ($\eta \sim 10^7$ p) in which the relaxation mechanism is different from that discussed above. Unfortunately, the same experimental techniques have not been successful with liquids of low viscosity ($\eta \sim 1$ cp), so that neither the magnitude nor the frequency dependence of shear moduli for such liquids have been measured. The only values available for comparison are those by Starunov *et al.*,[1] determined from the depolarized-doublet spectra discussed in this paper. Their values for nitrobenzene, aniline, and quinoline are 4.0×10^8, 3.1×10^9, and 1.2×10^9 dyn/cm^2, respectively. The disparities with the values listed in Table VII are due to differences in data analysis. Starunov *et al.*[1] approximated the shear-wave frequency ν_T by the observed doublet frequency ν_S, without taking into account the instrumental and theoretical line-profile effects discussed in Sec. IV A.

B. Shear Relaxation Time

It was shown in Sec. IV B that shear-wave relaxation times τ_μ (determined from doublet widths in I_H^V spectra) have the same values as anisotropy relaxation or molecular reorientation times τ_X (determined from Rayleigh linewidths in I_H^H spectra). Thus it is interesting to compare values of $\tau(\equiv \tau_\mu \equiv \tau_X)$ measured here, and listed in Table VII, with the extensive measurements of relaxation times in liquids carried out by dielectric-relaxation, nuclear-magnetic-resonance, and light-scattering techniques.

1. Dielectric Relaxation and Nuclear Magnetic Resonance

In Sec. II, we introduced expressions for the depolarized spectra derived from macroscopic fluctuation theory. Depolarized scattering may also be considered on a microscopic basis in terms of scattering from an ensemble of tumbling molecules.[17] The breadth of the depolarized spectrum is determined by the correlation time τ_2 of the molecular polarizability autocorrelation function, which is a second-rank tensor. By definition, τ_2 is the time for this function to decay to $1/e$ of its initial value, which occurs after a molecule has rotated through an angle of $\sim 30°$. The relaxation time τ_1 measured in a dielectric-relaxation experiment is determined by the dipole autocorrelation function[18] (a first-rank tensor), and is the time for a molecule to reorient through $\sim 60°$. Finally, for nuclear magnetic resonance, it is the spin-spin correlation function[18] which relaxes in time; this function is a second-rank tensor just as the polarizability autocorrelation function in light scattering.

The relation between the light scattering (or nuclear magnetic resonance) and dielectric-relaxation times depends on a number of factors and has been considered in detail by Montrose and Litovitz[19] and Ivanov.[20] The ratio τ_1/τ_2 depends primarily on the molecular symmetry and on the specific mechanism responsible for the relaxation. For most molecular geometries, the value $\tau_1/\tau_2 \gtrsim 2$ is indicative of molecular reorientation via a diffusion process; but if $\tau_1/\tau_2 \sim 1$, then reorientation occurs in large angular steps which occur every $\tau_1 \simeq \tau_2$ sec. The available values for the liquids investigated are given in Table VIII. It is noted that all but one of the values are $\lesssim 1$, indicating that reorientation in these liquids occurs in large rotational jumps.

Our values for the relaxation time are also compared with nuclear-magnetic-resonance data in Table VIII. The large differences in relaxation times are not understood, but may be due to measurements of reorientation times about different molecular axes in the two experiments.

2. Light Scattering

Two light-scattering techniques have been used to evaluate relaxation times, depolarized Rayleigh scattering of the type reported here and stimulated Rayleigh scattering. In the latter, a stimulated spectral line is observed shifted from the incident-light frequency by the frequency $1/\tau$, where τ is a characteristic reorientation time. The results of Cho *et al.*[21] are presented in Table VIII for nitrobenzene and *m*-nitrotoluene and are in close agreement with the values reported here.

Many investigations of depolarized Rayleigh scattering have been reported with mercury arc and, more recently, laser excitation. Diffraction gratings have been used successfully to analyze the broad "Rayleigh wings" but the resolution has been inadequate to obtain reliable values of linewidths, so that the relaxation times reported for the narrow component are too short and thus un-

TABLE VIII. Comparison with relaxation times τ' obtained from stimulated Rayleigh scattering,[a] depolarized Rayleigh-scattering[b] nuclear magnetic resonance,[c] and ratios of dielectric relaxation time and shear-wave relaxation times τ_1/τ_2.

Liquid	Temperature or Temp. range (°C)	τ (This work) 10^{-11} sec	τ' 10^{-11} sec	$\frac{\tau_1}{\tau_2}$	Ref.
Aniline	23	2.2	2.1[b]		23
	−6	7.2	5.0[c]		24
	20	2.4	2.0[c]		24
	20–40			0.8	25,27
Anisaldehyde	30			1.2	26
α-bromonaphthalene	20–55			1.0	27
α-chloronaphthalene	15–60			0.8	28,29
Benzonitrile	20–30			1.3	27
Benzyl benzoate	23			0.5	30
Bromobenzene	5	1.6	0.8[c]	1.2	31,28
Chlorobenzene	5	1.2	0.6[c]	1.1	24,28
Dibromo ethane	25			0.7	28
Diphenyl methane	30–60			3.0	32
m-dichlorobenzene	15			0.8	28
m-nitrotoluene	26	5.0	6.0[a,b]		21,22
Nitrobenzene	20	3.9	4.7[a]		21
	23	3.9	4.3[b]		22,23
	25	3.8	5.6[c]		33
	20–50			1.2	27,34
Quinoline	1–60			1.1	35
Tetralin	20	3.2	0.5[c]	0.9	29
1,2,4 trichlorobenzene	15–75			0.7	28

suitable for comparison. The results of more recent studies[22,23] with Fabry–Perot interferometers presented in Table VIII are found to compare well with our values. In a number of these experiments,[23] specifically those performed at scattering angles other than 180°, the resolution was insufficient to detect the depolarized doublets and the spectra were analyzed as simple Lorentzian lines. Nevertheless, since the inequality $\omega_T\tau \ll 1$ usually is satisfied, errors in τ are small and the agreement with our results is still good.

VIII. CONCLUSIONS

The present studies of light-scattering spectra have shown that many molecular liquids exhibit a depolarized doublet centered at the exciting frequency. The main criterion for its appearance is that the molecules must possess anisotropic polarizability. This molecular property provides the coupling between the incident light beam and rotational fluctuations of the molecules in the medium, which in turn are caused by heavily damped shear waves that propagate for distances of at most a few hundred angstroms. Such a mechanism had been proposed before the first observations of such spectra by Leontovich and in a more detailed theory by Rytov.

The observed line shapes, their dependence on the state of polarization, and their intensities are in quantitative agreement with Rytov's theory. Analyses of the observed spectra based on this theory have revealed a Brillouin-type dependence of the doublet splitting on scattering angle, indicating a propagating mode. The large widths of the observed doublets indicate very heavy damping of this mode. Values of the relaxation times for this mode have been determined and found to be $>10^{-11}$ sec, essentially the same as those measured in dielectric-relaxation experiments. From these measurements, values of the high-frequency shear modulus μ_∞ have been determined.

Two limitations of Rytov's theory have been noted. One is that the relation $\mu_\infty\tau/\eta = 1$ does not hold for the liquids studied, possibly implying that the total viscosity does not relax with a time τ. The other is the dispersion of the shear-wave frequency at low temperature observed in quinoline and aniline. Rytov's theory assumes a temperature-independent shear-wave frequency, which was corroborated for many of the liquids in this study. This discrepancy between theory and experiment in quinoline and aniline at low temperature is not understood, but it does suggest the inadequacy of the theory when the shear waves are not heavily damped.

Since the first reports of the observation of depolarized doublets, many theoretical papers have

appeared, notably by Ben-Reuven and Gershon,[36] Keyes and Kivelson,[37] Andersen and Pecora,[38] Ailawadi, Berne, and Forster,[39] and Chung and Yip.[40] Brief comparisons of the observed spectra presented here and the predictions of these new theories have already been made by us.[41] More detailed comparions must await further experimental results at higher resolution and possibly of simpler molecular liquids, as well as refinements in the recent theories.

---

*Research supported in part by the National Research Council of Canada and the University of Toronto. The work reported here is based on the thesis by G. I. A. Stegeman submitted for the Ph.D. degree to the University of Toronto. Brief preliminary reports of this work have been presented at meetings of the American Physical Society [Bull. Am. Phys. Soc. **14**, 74 (1969)], the Canadian Association of Physicists [Phys. Can. **25**, 26 (1969)], at the International Conference on Quantum Electronics [IEEE J. Quantum Electron. QE-4, 35 (1968)], and in Ref. 2.

[1]V. S. Starunov, E. V. Tiganov, and I. L. Fabelinskii, Zh. Eksp. Teor. Fiz. Pis'ma Red. **5**, 317 (1967) [JETP Lett. **5**, 260 (1967)].

[2]G. I. A. Stegeman and B. P. Stoicheff, Phys. Rev. Lett. **21**, 202 (1968).

[3]G. C. Knollman and A. S. Hamamoto, J. Chem. Phys. **47**, 5232 (1967).

[4]A. J. Barlow, J. Lamb, A. J. Matheson, P. R. K. L. Padmini, and J. Richter, Proc. Phys. Soc. Lond. A **298**, 461 (1967); Proc. Phys. Soc. Lond. A **298**, 481 (1967).

[5]L. Brillouin, J. Phys. (Paris) **4**, 153 (1936).

[6]M. A. Leontovich, Izv. Akad. Nauk SSSR Ser. Fiz. **5**, 148 (1941) [J. Phys. USSR **4**, 499 (1941)].

[7]S. M. Rytov, Zh. Eksp. Teor. Fiz. **33**, 514 (1957) [Sov. Phys.-JETP **6**, 401 (1958)].

[8]V. Volterra, Phys. Rev. **180**, 156 (1969).

[9]A. Sommerfield, *Mechanics of Deformable Bodies* (Academic, New York, 1964), p.106.

[10]See, for example, L. D. Landau and E. M. Lifshitz, *Statistical Physics* (Addison-Wesley, Reading, Mass., 1958), p. 374.

[11]G. I. A. Stegeman, W. S. Gornall, V. Volterra, and B. P. Stoicheff, J. Acoust. Soc. Am. **49**, 979 (1971).

[12]Tables II-IV give representative data only. A set of the complete tables has been deposited with the National Auxiliary Publications Service of the American Society for Information Service, NAPS No. 02008.

[13]An alternate form for μ has been given by M. A. Isakovich and I. A. Chaban, Zh. Eksp. Teor. Fiz. **50**, 1343 (1966) [Sov. Phys.-JETP **23**, 893 (1966)].

[14]S. L. Shapiro and H. P. Broida, Phys. Rev. **154**, 129 (1967); H. C. Craddock, D. A. Jackson, and P. G. Powles, Mol. Phys. **14**, 1 (1968).

[15]W. S. Gornall, H. E. Howard-Lock, and B. P. Stoicheff, Phys. Rev. A **1**, 1288 (1970).

[16]V. G. Roth, Z. Naturforsch. 18, A516 (1963).

[17]R. Pecora and W. A. Steele, J. Chem. Phys. 42, 1872 (1965).

[18]W. A. Steele, J. Chem. Phys. **38**, 2404 (1963).

[19]C. J. Montrose and T. A. Litovitz, *Neutron Inelastic Scattering* (International Atomic Energy Commission, Vienna, 1968), Vol.1, p. 623.

[20]E. N. Ivanov, Zh. Eksp. Teor. Fiz. **45**, 1509 (1963) [Sov. Phys.-JETP **18**, 1041 (1964)].

[21]C. W. Cho, N. D. Foltz, D. H. Rank, and T. A. Wiggins, Phys. Rev. Lett. **18**, 107 (1967).

[22]A. Szöke, E. Courtens, and A. Ben-Reuven, Chem. Phys. Lett. **1**, 87 (1967).

[23]H. C. Craddock, D. A. Jackson, and J. G. Powles, Mol. Phys. **14**, 1 (1968).

[24]J. G. Powles and D. J. Neale, Proc. Phys. Soc. Lond. **78**, 377 (1961).

[25]S. K. Garg and C. P. Smyth, J. Chem. Phys. **46**, 373 (1967).

[26]A. Bhanumathi, Indian J. Pure Appl. Phys. **1**, 79 (1963).

[27]E. Fischer, Z. Phys. **127**, 49 (1949).

[28]J. Bhattacharyya, S. B. Roy, and G. S. Kastha, Indian J. Phys. **40**, 187 (1966).

[29]R. W. Rampolla and C. P. Smyth, J. Am. Chem. Soc. **80**, 1057 (1958).

[30]K. Symalamba and D. Premaswarup, Indian J. Pure Appl. Phys. **3**, 243 (1965).

[31]J. G. Powles and R. Figgins, Mol. Phys. **13**, 253 (1967).

[32]E. N. Dicarlo and C. P. Smyth, J. Am. Chem. Soc. **84**, 3638 (1962).

[33]W. B. Moniz and H. S. Gutowsky, J. Chem. Phys. **38**, 1155 (1963).

[34]P. Girard and P. Abodie, Trans. Faraday Soc. **42**, 40 (1946); A. J. Curtis, P. L. McGeer, G. I. Rathman, and C. P. Smyth, J. Am. Chem. Soc. **74**, 644 (1952); E. Fischer and R. Fessler, Z. Naturforsch. 8, A177 (1953).

[35]R. S. Holland and C. P. Smyth, J. Phys. Chem. **59**, 1088 (1955); R. C. Miller and C. P. Smyth, J. Am. Chem. Soc. **79**, 308 (1957).

[36]A. Ben-Reuven and N. D. Gershon, J. Chem. Phys. **54**, 1049 (1971).

[37]T. Keyes and D. Kivelson, J. Chem. Phys. **54**, 1786 (1971).

[38]H. C. Andersen and R. Pecora, J. Chem. Phys. **54**, 2584 (1971).

[39]N. K. Ailawadi, B. J. Berne, and D. Forster, Phys. Rev. A **3**, 1472 (1971).

[40]C. H. Chung and S. Yip, Phys. Rev. A **4**, 928 (1971).

[41]G. D. Enright, G. I. A. Stegeman, and B. P. Stoicheff, J. Phys. (Paris) 33, 207 (1972).